J. Phys. B: At. Mol. Opt. Phys. **21** (1988) 1237-1254. Printed in the UK

Resonant vibrational excitation of N_2 by electron impact in the 15–35 eV energy range

L Malegat and M Le Dourneuf

ER 261 du CNRS, Observatoire de Paris, 92195 Meudon, France

Received 27 August 1987, in final form 30 December 1987

Abstract. We present parameter-free differential and integral cross sections for the vibrational excitation of N_2 by electron impact in the 15-35 eV range, which is dominated by a $^2\Sigma_u$ shape resonance. Our calculation is based on a static+exact exchange+local polarisation-correlation approximation of the electron-molecule interaction and on the adiabatic-nuclei approximation for the coupling with the nuclear motion. Our fixed-nuclei results agree reasonably well with the single previous *ab initio* calculation of Burke *et al.* However, more detailed vibrational results allow us to point out two specific features of the intermediate-energy $^2\Sigma_u$ resonance. First, it originates from the *resonant variation of a single fixed-nuclei 'diabatised' eigenphase*, which corresponds to a nearly constant mixing of p, f partial waves with dominant f character, in agreement with the previous qualitative assessments of Dehmer *et al* and Chang. Second, the various vibrational excitation cross sections peak at notably different energies, owing to the combined effect of the broad resonance pole and the Franck-Condon factors. Finally, the remaining discrepancy (2-4 eV) between all the calculated and observed resonant peaks is discussed, and attributed primarily to the neglect of inelasticity and the approximate treatment of correlations.

1. Introduction

The first evidence of a resonant enhancement in the vibrational excitation of N_2 by electron impact about 22 eV was reported by Pavlovic *et al* (1972): the large width of the phenomenon (6-7 eV) and the complex energy dependence of the vibrational differential cross sections (DCS) suggested that it may result from the overlap of many short-lived shape, as well as core-excited Feshbach resonances. However, in 1980, Dehmer *et al*, using a simple theory—adiabatic nuclei approximation for the nuclear motion, continuum-multiple-scattering model for the fixed-nuclei electronic scattering—showed that a single σ_u shape resonance could reproduce the observed enhancement. Additional work remained necessary to understand the rapid energy variation of the measured DCS and to improve the accuracy of the calculation. New measurements (Tronc *et al* 1980, Tanaka *et al* 1981), producing DCS with a slow energy variation, brought controversy. Chang (1983) related these different energy variations to different experimental energy resolutions: the 30 meV resolution of Pavlovic *et al* excluded more rotational branches ($\Delta j = 4, 6$) than the 50 meV resolution of the later two measurements (only partly $\Delta j = 6$). However, Chang's explanation relied on a two-channel approximation with a constant mixing of p, f partial waves in the eigenphases. This last assumption was questioned by Burke *et al* (1983, hereafter referred to as BNS), who presented, for the first time, *ab initio* multicentre R-matrix results, including exchange exactly and polarisation approximately through particle-hole-type discrete excitations. They

0953-4075/88/071237+18$02.50

pointed out a strong R dependence of the p-f mixing, but did not explicitly study its influence on the vibrational DCS. They also related the remaining discrepancy between the calculated and observed resonance positions to an improper account of inelasticity, a possibly incomplete representation of polarisation and a complete neglect of the target electronic correlations. The last effect has been investigated on the fixed-nuclei elastic scattering by Rumble *et al* (1984), using a static+model exchange potential with correlated target density, and by Weatherford *et al* (1987) using a correlated static potential+SCF non-local exchange+local polarisation interaction. In spite of the approximate nature of both investigations, they suggest that the target correlation only marginally affects the $^2\Sigma_u$ cross section above 20 eV for the two relevant internuclear distances studied ($R_{eq} = 2.068\ a_0$ and $R = 2.45\ a_0$).

In the present paper, we report parameter-free results of an adiabatic-nuclei single-centre close-coupling calculation, including exact exchange through a separable expansion (Malegat *et al* 1987) and approximate polarisation through a free-electron-gas correlation-polarisation potential (O'Connell and Lane 1983, Padial and Norcross 1984). The theoretical approach is outlined in § 2. Three aspects of our fixed nuclei results are discussed in § 3: the sensitivity of the $^2\Sigma_u$ scattering to the representation of exchange and polarisation in § 3.1, its approximate description by two uncoupled diabatised channels (an f-dominant resonant one and a p-dominant non-resonant one) in § 3.2 and the relative contributions of the other symmetries in § 3.3. In § 4, we bring out three aspects of our adiabatic nuclei calculation. First, the vibrational averaging leads to vibrational excitation cross sections whose magnitudes decrease rapidly with increasing Δv, and whose shapes are strongly influenced by Franck-Condon effects (§ 4.1). Second, their comparison with the accurate total cross sections (Kennerly 1980) and the fixed-angle vibrational excitation DCS (Tanaka *et al* 1981, Tronc 1983, Tronc and Malegat 1985), obviously relates the theoretical overestimate of the peak positions (2-4 eV) to the neglect of inelasticity; however, after a proper renormalisation of the energy scale, the comparison of our vibrational excitation DCS with the low-resolution relative measurements of Tronc *et al* shows that our calculation accurately predicts the angular properties of the $^2\Sigma_u$ resonance (§ 4.2). We are then in a position to prove that the $N_2^-(^2\Sigma_u)$ resonant vibrational DCS are described within 10% by Chang's (1983) two-wave model with constant mixing angle, provided that his original formula is corrected for missing interference terms, and that it is used with a mixing angle quite different from the one he proposed (§ 4.3). In the appendix, we carefully correct his simple formula, which gives the angular dependence of the resonant vibrational DCS in terms of the two-wave mixing angle. This formula, involving a single, physically meaningful, parameter, can be quite useful in the experimental analysis of intermediate energy resonances in homonuclear diatomics, provided that Chang's basic assumption—definition of a single high-l resonant eigenphase by 'diabatisation' of its avoided crossing with a non-resonant lower-l eigenphase—is valid. In § 5, we summarise our present knowledge on the $N_2^-(^2\Sigma_u)$ shape resonance and discuss directions for future work.

2. Theoretical approach

2.1. Method

To study the e-N_2 scattering in the intermediate energy range (15-35 eV) dominated by the broad $^2\Sigma_u$ shape resonance in the elastic electronic channel, we use the adiabatic-

nuclei (AN) formalism (Chase 1956) in its energy-modified improved form (Nesbet 1979). The calculation then proceeds in two steps.

In the first step, the fixed-nuclei (FN) elastic e-N_2 scattering is studied as a function of internuclear distance R, using the single-centre close-coupling formalism. A single target state, the N_2 ($X\ ^1\Sigma_g^+$) ground electronic state, is included using Nesbet's (1964) near-Hartree-Fock wavefunction as BNS did. The scattered electron wavefunction is expanded in spherical partial waves with respect to the centre of mass of the N_2 target. Exchange is included exactly in the resonant σ_u symmetry, by expansion of the exchange kernel on a finite L^2 basis of Slater-type orbitals (Malegat *et al* 1987), and approximately in the other symmetries, through the Hara free-electron-gas (HFEG) local potential. The explicit orthogonalisation to the N_2 closed-shell orbitals is imposed in both cases. The σ_u exchange basis is derived from Nesbet's molecular basis, by adding short-ranged functions at the nuclei and at the centre of mass, in order to describe the compact resonant σ_u orbital accurately: it is given in table 1 for R_{eq} and deduced at other internuclear distances by scaling the exponents of the centre-of-mass orbitals as R_{eq}/R. Polarisation is included using the variational form (Padial and Norcross 1984) of the local-density correlation-polarisation potential (O'Connell and Lane 1983), with the uniform-electron-gas correlation energy given by Vosko *et al* (1980), and the R-dependent polarisabilities calculated by Morrison and Hay (1979) in the perturbed Hartree-Fock approximation.

Table 1. Slater-type orbitals used in the separable exchange approximation.

Nuclei-centred						CDM-centred	
nl	Exponent (a_0^{-1})	nl	Exponent (a_0^{-1})	nl	Exponent (a_0^{-1})	nl	Exponent (a_0^{-1})
1s	6.212 92	2p	1.528 53	3d	1.935 00	2p	10.000 00
	9.368 27		2.127 66		2.437 00		5.000 00
2s	1.467 86		3.336 78				3.333 33
	1.785 71		6.666 66			4f	20.000 00
	2.246 42						12.000 00
	3.333 33						

In the second step, each vibrational $T^{\lambda}_{v_i l_i v_f l_f}(E)$ matrix element is deduced by vibrational averaging:

$$T^{\lambda}_{v_i l_i v_f l_f}(E) = \int \mathrm{d}R\, \chi_{v_i}(R)\, T^{\lambda}_{l_i l_f}(R; E)\, \chi_{v_f}(R) \tag{1}$$

from the corresponding FN $T^{\lambda}_{l_i l_f}(R; E)$ matrix element for the projection λ of the scattered electron's angular momentum along the internuclear axis. The target vibrational functions $\chi_v(R)$ are calculated in a Morse potential $V(R) = D(1 - \mathrm{e}^{-\alpha(R-R_0)})^2$ whose parameters $D = 11.9134$ eV, $R_0 = 2.0743\ a_0$ and $\alpha = 1.297\,45\ a_0^{-1}$ are adjusted to reproduce exactly the $v = 1$ and $v = 20$ vibrational levels of N_2 (Lofthus 1960), a maximal deviation of about 2 meV occurring for $v = 15$ (Launay 1987).

The integral vibrational cross sections are given by

$$\sigma_{v_i v_f}(\tfrac{1}{2}k_i^2) = \frac{\pi}{k_i^2} \sum_{\lambda \geq 0 l_i l_f} \frac{2}{1 + \delta_{\lambda 0}} |T^{\lambda}_{v_i l_i v_f l_f}(\tfrac{1}{2}k_i k_f)|^2 \tag{2}$$

where $\frac{1}{2}k_ik_f$ is the geometrical average of the electronic kinetic energies in the initial and final vibrational channels (Nesbet 1979).

Following Fano and Dill (1972), by introducing the momentum transferred from the target to the scattered electron $\boldsymbol{j}_t = \boldsymbol{l}_f - \boldsymbol{l}_i$, the vibrational DCS can be expressed as incoherent superpositions of standard geometrical functions $\Theta(j_t; l_il_i'l_fl_f'; \theta)$, weighted by dynamical factors $\tau^{j_t}_{v_il_iv_fl_f}$. In the simple case of a $^1\Sigma^+$ target state, the scattering angle θ being defined with respect to the incident beam direction, the vibrational excitation DCS can be written

$$\sigma_{v_iv_f}(\theta) = \frac{\pi}{k_i^2} \sum_{\substack{\bar{j}_t \\ l_il_i'l_fl_f'}} i^{l_i-l_f-l_i'+l_f'}[(2l_i+1)(2l_i'+1)]^{1/2}\Theta(j_t; l_il_i'l_fl_f'; \theta)\tau^{j_t}_{v_il_iv_fl_f}\tau^{j_t}_{v_il_iv_fl_f}{}^* \tag{3a}$$

$$\Theta(j_t; l_il_i'l_fl_f'; \theta) = (-1)^{j_t}(2j_t+1)\frac{[(2l_f+1)(2l_f'+1)]^{1/2}}{4\pi}$$

$$\times \sum_k \begin{Bmatrix} l_i' & l_i & k \\ l_f & l_f' & j_t \end{Bmatrix} (l_i0, l_i'0|k0)(l_f0, l_f'0|k0)P_k(\cos\theta) \tag{3b}$$

$$\tau^{j_t}_{v_il_iv_fl_f} = \sum_{\lambda \geqslant 0} (-1)^{l_i+\lambda}\frac{2}{1+\delta_{\lambda 0}}\begin{pmatrix} l_i & l_f & j_t \\ \lambda & -\lambda & 0 \end{pmatrix} T^{\lambda}_{v_il_iv_fl_f}. \tag{3c}$$

In (3*a*), the notation $\bar{j}_t$ indicates a restricted summation over j_t values satisfying the 'parity-favoured' condition ($l_i + l_f + j_t$ even), which ensures the conservation of the total parity.

2.2. Numerical implementation

The scattering calculation has been performed by De Vogelaere integration of the set of coupled inhomogeneous second-order differential equations (Malegat *et al* 1987), using the code PARSEP (Vo Ky Lan 1984).

FN eigenphases converged to 2×10^{-2} rad are obtained:

(1) by including angular momenta up to $l_{max} = 30$ in the single-centre expansion of the molecular and scattered electron orbitals, and up to $2l_{max}$ in that of the interaction potential,

(2) by using an integration grid with a variable stepsize ranging from $h_{min} = 0.008(R/R_{eq})a_0$ near the nuclei, to $h_{max} = 0.256(R/R_{eq})a_0$ in the asymptotic region and

(3) by integrating the coupled radial equations up to $r_{max} = 10(R/R_{eq})a_0$.

The reliability of these parameters has been established by checking that neither an extension of the single-centre expansions up to $l_{max} = 40$, nor an extended propagation of the K matrix up to $r_{max} = 100\ a_0$ using the variable-phase method (Le Dourneuf and Vo Ky Lan 1977) significantly affects the results, even for the most sensitive resonance parameters.

Vibrational excitation cross sections between $v = 0, 1, 2$ numerically accurate to $10^{-3}\ a_0^2$ are obtained in three steps.

(1) The FN calculation is repeated for 13 internuclear distances, ranging from 1.768 to 2.468 a_0 to cover the spatial extent of the first three vibrational functions, using an R grid with a constant step of 0.05 a_0 from 1.868 to 2.368 a_0 to account for the rapid variation of the $T^{\sigma_\mu}_{l_il_f'}(R; E)$ matrix elements.

(2) The $\chi_v(R)$ functions and $T^{\sigma}_{l_i l_f}(R, E)$ matrix elements are interpolated by spline functions of third order.

(3) The R integration of equation (1) is achieved using composite Gauss-Legendre quadratures with seven equal sectors between 1.768 and 2.468 a_0 and 6-10 Gauss points in each sector.

3. Fixed-nuclei elastic scattering results

3.1. Sensitivity of the FN results to the description of exchange and polarisation

Within the one-electronic-target-state close-coupling approximation, we have investigated the sensitivity of the FN results to the accuracy of the electron-molecule interaction. In the 15-35 eV energy range, it appears most clearly in the resonant $^2\Sigma_u$ symmetry.

Figure 1(a) shows the variation of the $^2\Sigma_u$ eigenphase sum with energy at R_{eq} under various approximations: $S_\perp$ stands for the inclusion of the static interaction and the orthogonalisation to the target-occupied orbitals, E_M for that of the HFEG model exchange, E_X for that of the exact separable exchange and P_M for that of the model correlation-polarisation potential. In the $S_\perp$ approximation, the attraction is too weak to induce a resonance below 35 eV. The model $S_\perp E_M$ and exact $S_\perp E_X$ static-exchange results agree closely, in contrast with their divergence for the low-energy $^2\Pi_g$ resonance at R_{eq}: $E_r = 5.42$ eV with HFEG exchange (Morrison and Collins 1978), $E_r = 3.83$ eV with exact exchange (Malegat *et al* 1987). This improvement of the HFEG model is not surprising, since the plane-wave approximation in the exchange kernel, which is an essential underlying assumption of the HFEG model, becomes more realistic as

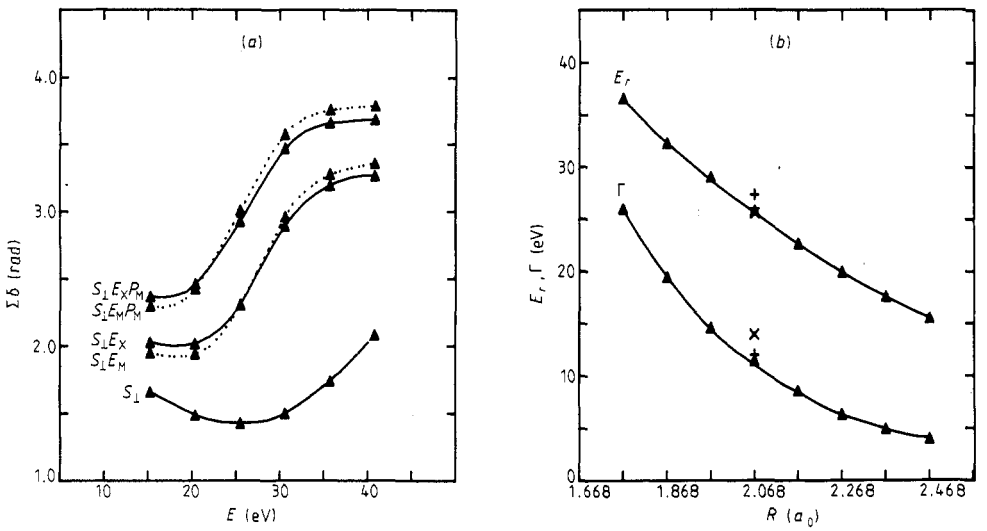

Figure 1. Fixed nuclei resonant results. (a) Σ_u eigenphase sum (rad) against energy (eV) at $R_{eq} = 2.068\ a_0$ under various approximations: $S_\perp$ = static+orthogonalisation to the occupied target orbitals; E_X = exact exchange; E_M = HFEG model exchange; P_M = model polarisation. ▲, calculated points; (——) and (· · · ·), interpolated curves. (b) Position (upper curve) and width (lower curve) of the $^2\Sigma_u$ resonance (eV) against internuclear distance (a_0). ▲, present $S_\perp E_X P_M$; +, present $S_\perp E_X$; ×, $S_\perp E_X$ from Burke *et al* (1983).

energy increases. The inclusion of polarisation enhances the $S_\perp E_M P_M$ and $S_\perp E_X P_M$ eigenphase sums by about 0.5 rad, whatever the energy.

More precisely, the position E_r and width Γ of the resonance are obtained by fitting the eigenphase sum to a Breit-Wigner formula plus a second-order polynomial. The accuracy is estimated to 0.25 eV for E_r and 0.50 eV for Γ at R_{eq}, by varying the number of energies in the fit. Figure 1(b) shows that, at the $S_\perp E_X P_M$ level, E_r and Γ decrease rapidly with internuclear distance R and that, at the $S_\perp E_X$ level for R_{eq}, our position is 1.8 eV higher than the BNS one, while our width is 2 eV lower (table 2). These opposite variations of $E_r(R_{eq})$ and $\Gamma(R_{eq})$ in two calculations using the same physical approximations and the same target wavefunction (Nesbet 1964) is surprising and most likely reflects limited numerical accuracies: since we have checked that neither the extension of the single-centre expansions nor that of the integration grid would significantly reduce the actual discrepancy, we are led to question either the convergence of the L^2 expansions and/or the accuracy of the BNS fit. On the other hand, the inclusion of our model polarisation potential hardly changes Γ, but lowers E_r by 1.6 eV, in close agreement with the 1.5 eV lowering reported by BNS when they include particle-hole discrete excitations.

Table 2. Position and width of the $^2\Sigma_u$ shape resonance (eV).

	$S_\perp E_X$ (BNS)	$S_\perp E_X$ (present)	$S_\perp E_X P$ (present)
E_r (R_{eq})	25.5	27.3	25.7
Γ_r (R_{eq})	13.9	11.9	11.7

3.2. Two-wave simplified description of the FN resonance

In the 15-35 eV energy range, the $^2\Sigma_u$ scattering is largely dominated by the contributions of the first two p,f partial waves.

Figure 2(a) illustrates the energy variation of the corresponding FN eigenphases (squares) and mixing angle β (triangles) at R_{eq}. The latter is the angle of the plane rotation that diagonalises the 2×2 S matrix. It is defined modulo $\pi/2$ and the largest mixing between the two orthogonal partial waves occurs for $\beta = \pi/4$. The two eigenphases show a narrow avoided crossing in the range of the broad resonance and, consequently, β presents a sharp variation of $-\pi/2$, which corresponds to the exchange of the two eigenvectors. It is superimposed on a small, slowly increasing background. The narrowness of the avoided crossing suggests considering 'diabatised' crossing eigenphases (dotted curves), which have nearly pure p or f characters and correspond to a small, slowly increasing mixing angle (full curve): they correspond to the eigenvectors of the time delay matrix (Wigner 1955) as suggested by Burke *et al* (1969) in the e-He case.

To assess the validity of this diabatisation, we have compared the results of the exact two-channel FN calculation with those of its diabatised counterpart, at three energies along the avoided crossing: 10.2 eV (far below), 26.8 eV (centre of the avoided crossing) and 40.8 eV (far above). The integral FN elastic cross sections differ by $0.1a_0^2$ at most at the crossing, but their relative variation remains less than 1%. Consequently,

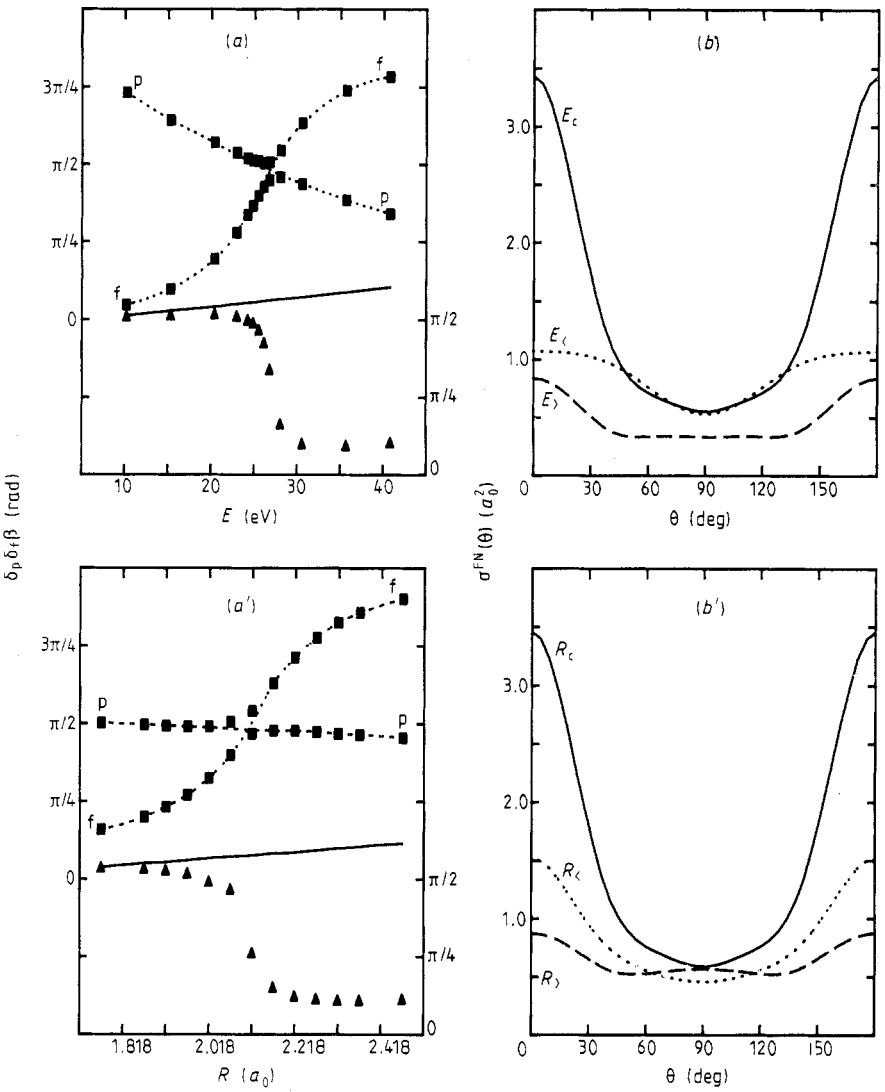

Figure 2. Fixed-nuclei resonant two-channel scattering model. (*a*) Eigenphases δ_p, δ_f (■) and mixing angle β (▲) in rad against energy in eV at $R_{eq} = 2.068\ a_0$. (· · · ·), diabatised eigenphases; (——), diabatised mixing angle. (*b*) Differential cross sections (a_0^2) at $R_{eq} = 2.068\ a_0$ for various energies. (· · · ·), $E_< = 0.375$ au, i.e. far below the crossing; (——), $E_c = 0.984\,375$ au, i.e. at the crossing; (- - -), $E_> = 1.5$ au, i.e. far above the crossing. The exact and diabatised curves are quasi-indistinguishable. (*a'*) δ_p, δ_f and β (rad) against internuclear distance (a_0) at $E_r \simeq 25.7$ eV. (*b'*) Differential cross sections (a_0^2) at $E_r \simeq 25.7$ eV for various internuclear distances. (· · · ·), $R_< = 1.768$ au, i.e. far below the crossing; (——), $R_c = 2.118$ au, i.e. at the crossing; (- - -), $R_> = 2.468$ au, i.e. far above the crossing.

the two calculations lead to indistinguishable FN elastic DCS on the scale of figure 2(*b*). However, the shape of the DCS changes significantly in the 10.2–40.8 eV energy range, evolving from a p-dominant character at low energy, to an f-dominant character at high energy, while its magnitude is maximal at E_r.

Figures 2(a') and 2(b'), which illustrate the variations of the same quantities (eigenphases, mixing angle, DCS) with the internuclear distance R at fixed energy $E_r(R_{eq}) = 25.7$ eV, suggest similar comments. Therefore, BNS remark about the practical importance of the avoided crossing may be questioned: we will precisely examine its effect on the AN vibrational excitation cross sections in § 4.3.

3.3. Importance of the various symmetries on the FN elastic cross section

Figure 3(a) displays the integral FN elastic cross section at R_{eq} (full curve) and the partial contributions (dotted curves) of the various symmetries (σ_g, σ_u, π_u, π_g, δ_g, δ_u, ϕ_u, ϕ_g) in the 15-35 eV range. The corresponding values are given in table 3. The σ_g contribution, which largely dominates the low-energy region, decreases steadily in this higher energy range. The σ_u symmetry culminates and varies the most strongly in this range, due to the broad resonance. All the higher symmetries remain controlled by centrifugal effects, which can be characterised by the minimal angular momentum allowed l_{min}. Note that $l_{min} = 0, 1, 1, 2, 2, 3, 3, 4$ respectively for the eight symmetries listed above. The corresponding partial cross sections increase slowly with energy, and decrease in magnitude for increasing l_{min}. These results qualitatively agree with previous FN calculations (Dill and Dehmer 1977, Rumble *et al* 1981, 1984).

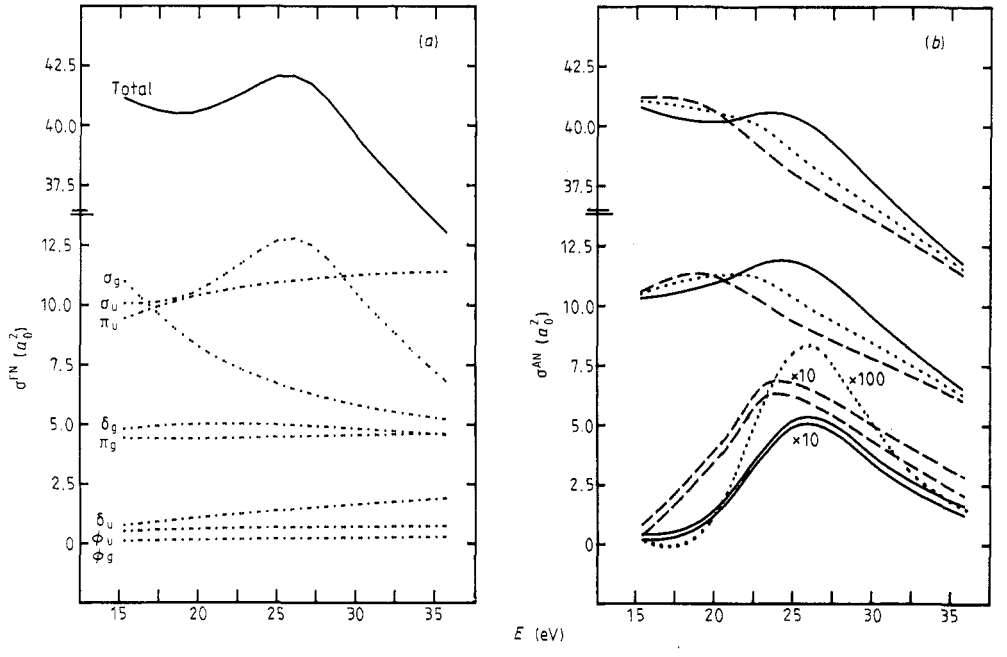

Figure 3. Comparison between fixed and adiabatic nuclei results. (a) Total (——) and partial (· · · ·) cross sections (a_0^2) against energy (eV) at $R_{eq} = 2.068\ a_0$. (b) Elastic and inelastic total and resonant cross sections (a_0^2) against energy (eV). Upper set of curves: total elastic; medium set of curves: resonant elastic; lower set of curves: total and resonant inelastic. (——), σ_{00} and $10 \times \sigma_{01}$; (· · · ·), σ_{11} and $100 \times \sigma_{02}$; (- - -), σ_{22} and $10 \times \sigma_{12}$.

Table 3. Partial and total integrated fixed nuclei elastic cross sections (a_0^2) against energy (eV).

E (eV)	Σ_g	Π_g	Δ_g	Φ_g	Σ_u	Π_u	Δ_u	Φ_u	Total
16	10.530	4.411	4.847	0.117	10.066	9.611	0.812	0.533	40.928
17	9.888	4.402	4.904	0.127	10.093	9.839	0.880	0.555	40.688
18	9.290	4.396	4.953	0.136	10.176	10.051	0.947	0.576	40.525
19	8.750	4.395	4.991	0.145	10.340	10.241	1.013	0.595	40.471
20	8.280	4.400	5.015	0.155	10.612	10.406	1.078	0.612	40.557
21	7.884	4.412	5.024	0.164	10.996	10.542	1.142	0.626	40.790
22	7.533	4.426	5.025	0.173	11.417	10.663	1.204	0.640	41.081
23	7.230	4.441	5.018	0.183	11.860	10.767	1.264	0.651	41.414
24	6.956	4.457	5.005	0.192	12.327	10.861	1.322	0.661	41.785
25	6.714	4.474	4.987	0.201	12.686	10.944	1.379	0.670	42.055
26	6.496	4.490	4.963	0.209	12.787	11.020	1.435	0.678	42.079
27	6.302	4.506	4.934	0.217	12.567	11.089	1.489	0.685	41.791
28	6.127	4.520	4.901	0.225	12.055	11.150	1.543	0.693	41.214
29	5.968	4.535	4.864	0.233	11.307	11.206	1.595	0.700	40.410
30	5.825	4.549	4.824	0.240	10.504	11.255	1.646	0.706	39.553
31	5.696	4.562	4.782	0.247	9.795	11.297	1.696	0.712	38.787
32	5.578	4.574	4.739	0.254	9.127	11.331	1.744	0.718	38.062
33	5.470	4.586	4.694	0.260	8.475	11.357	1.790	0.723	37.353
34	5.371	4.598	4.648	0.267	7.845	11.376	1.835	0.728	36.665
35	5.280	4.609	4.601	0.273	7.240	11.389	1.879	0.732	36.003

4. Adiabatic-nuclei results

4.1. Integrated vibrational cross sections

Figure 3(b) shows the vibrationally elastic and inelastic cross sections deduced from the present FN calculation, using (2) for $v \leqslant 2$. The three elastic cross sections $0 \rightarrow 0$, $1 \rightarrow 1$, $2 \rightarrow 2$ (upper set of curves) have shapes and magnitudes similar to the FN elastic cross section (figure 3(a)), the σ_u resonance appearing as a mere hump over a rapidly decreasing background. However, the vibrational averaging lowers the peak position and broadens it, increasingly so for increasing v. As to the vibrational excitation cross sections, they are dominated by the σ_u symmetry (see also table 4), since the R averaging of the T matrix elements over a product of two orthogonal vibrational functions almost eliminates the weakly R-dependent non-resonant contributions. When Δv increases from 1 to 2, the resonant contribution becomes completely dominant, while the absolute value of the cross section decreases by nearly one order of magnitude. The different cross sections peak at notably different energies. This reflects the combined effects of the broad resonance pole and the Franck-Condon overlaps in determining the profile of each cross section. Thus, the peak positions determined on individual cross sections do not correspond to the resonance position, deduced theoretically from a Breit-Wigner fit of the FN eigenphase sum. Correctly speaking, the comparison between experiment and theory should only involve peak positions in specific cross sections.

Figure 4 compares our integrated vibrational excitation cross sections with previous calculations. The peak positions and shapes of the two more detailed studies (the present ones in full curves, Dehmer *et al*'s (1980) results in dotted curves) agree closely. As to the magnitudes of the cross sections, ours are somewhat smaller, but agree closely with the two energy points ($E = 20, 30$ eV) of Rumble *et al* (1981), who

Table 4. Total and partial (Σ_u) integrated vibrational cross sections $\sigma_{vv'}$ (a_0^2) against energy (eV).

$\sigma_{vv'}$ (a_0^2)	σ_{00}	σ_{11}	σ_{22}	σ_{01}		σ_{02}		σ_{12}	
E (eV)	Total	Total	Total	Σ_u	Total	Σ_u	Total	Σ_u	Total
16	40.612	40.996	41.201	0.018	0.041	0.000	0.000	0.070	0.116
17	40.421	40.918	41.193	0.024	0.047	0.000	0.000	0.134	0.180
18	40.281	40.817	41.114	0.041	0.063	0.001	0.001	0.202	0.248
19	40.199	40.699	40.928	0.072	0.094	0.004	0.004	0.274	0.320
20	40.181	40.569	40.600	0.122	0.145	0.012	0.012	0.347	0.394
21	40.256	40.434	40.125	0.194	0.218	0.024	0.024	0.425	0.473
22	40.440	40.259	39.611	0.281	0.305	0.041	0.041	0.527	0.577
23	40.567	39.948	39.075	0.365	0.391	0.057	0.058	0.613	0.664
24	40.568	39.474	38.517	0.441	0.467	0.071	0.072	0.633	0.689
25	40.410	38.948	38.034	0.495	0.522	0.080	0.081	0.631	0.679
26	40.080	38.433	37.609	0.509	0.538	0.084	0.084	0.597	0.654
27	39.601	37.969	37.208	0.493	0.522	0.080	0.080	0.562	0.622
28	39.015	37.533	36.820	0.455	0.486	0.070	0.071	0.524	0.587
29	38.357	37.096	36.448	0.403	0.435	0.061	0.061	0.482	0.547
30	37.677	36.658	36.085	0.345	0.378	0.051	0.051	0.437	0.504
31	37.040	36.217	35.708	0.295	0.329	0.042	0.042	0.394	0.463
32	36.429	35.769	35.319	0.252	0.287	0.034	0.034	0.353	0.425
33	35.834	35.314	34.922	0.213	0.250	0.027	0.028	0.314	0.387
34	35.255	34.854	34.518	0.179	0.216	0.022	0.023	0.275	0.351
35	34.691	34.389	34.107	0.148	0.186	0.018	0.018	0.234	0.315

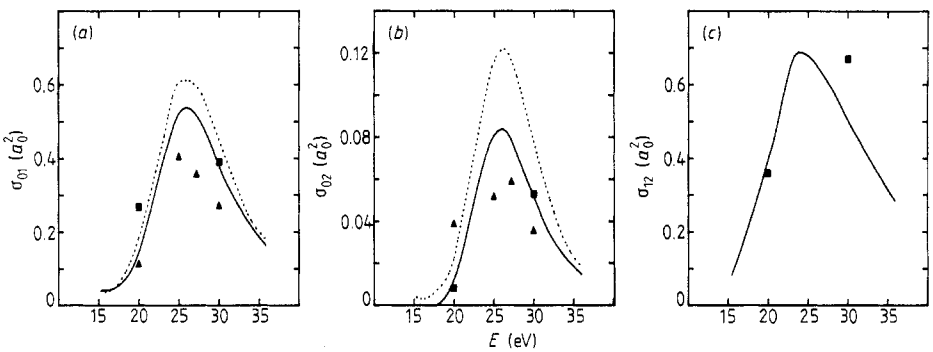

Figure 4. Integrated cross sections for vibrational excitation. (*a*) σ_{01} in a_0^2 against energy in eV; (——), present work; (· · · ·), Dehmer *et al* (1980); ■, Rumble *et al* (1981); ▲, Burke *et al* (1983). (*b*) Same as (*a*) but for 0→2 excitation. (*c*) Same as (*a*) but for 1→2 excitation.

used a slightly simpler physical approximation (static potential + HFEG exchange + adiabatic polarisation with the standard exponential cut-off). By contrast, the adiabatic nuclei R-matrix cross sections of BNS are smaller; however, the irregularity of their shapes suggests a numerical inaccuracy, which may originate from a cumbersome averaging over intermediate-energy pseudoresonances (Burke 1987). As a conclusion of these theoretical comparisons, it seems that all the current calculations, based on similar physical models (static exchange + polarisation), lead to similar peak shapes and positions.

4.2. Total and vibrational excitation cross sections compared with accurate experiments

In figure 5(*a*), our total FN (dotted curve) and AN (full curve) cross sections are compared with the 3% accuracy absolute data from a transmission time-of-flight experiment (triangles, Kennerly 1980). Note that our FN data are obtained at the experimental equilibrium position $R_{eq} = 2.068\ a_0$, while our AN ones result from an R averaging over the molecular wavefunction of Nesbet (1964), that yields the value $2.026\ a_0$ for the equilibrium position. Although our peak position is lowered by about 5 eV in the R-averaging procedure, our AN electronically elastic peak remains about 2 eV higher than the experimental one. This overestimation of the resonant peak position, combined with the underestimation of our total cross section by about 10%, clearly originates from the neglect of electronic excitation.

In figure 5(*b*), our fixed-angle vibrational excitation DCS $\sigma_{01}(\theta = 90°)$ is compared with the absolute experimental values of Tronc *et al* (1983, 1985, dotted curve) and Tanaka *et al* (1981, triangles). Our peak position ($E_r^{th} \simeq 25.5$ eV) and our full width at half maximum ($\Gamma^{th} \simeq 10$ eV) are also larger than the experimental values ($E_r^{exp} \simeq 22$ and 21 eV, $\Gamma^{exp} \simeq 7.5$ and 7 eV respectively). This allows us to recalibrate the energy scale, using the reduced energy $E_{red} = 2(E - E_r)/\Gamma$, in order to achieve a meaningful comparison with relative experimental DCS.

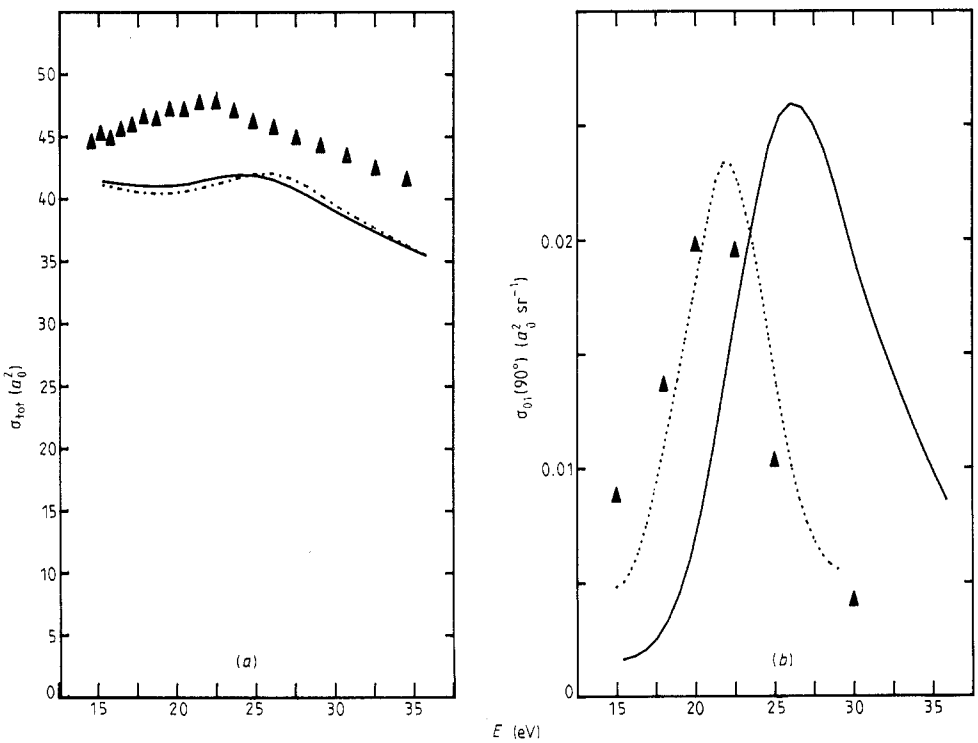

Figure 5. Total integrated and $0 \rightarrow 1$ vibrational excitation differential cross sections. (*a*) Total cross sections (a_0^2) against energy (eV). (——), present $\sigma_{00} + \sigma_{01} + \sigma_{02}$; (· · · ·), present FN cross section; ▲, Kennerly (1980). (*b*) $\sigma_{01}(90°)$ in a_0^2 against energy in eV; (——), present work; ▲, Tanaka *et al* (1981); (· · · ·), Tronc *et al* (1983, 1985).

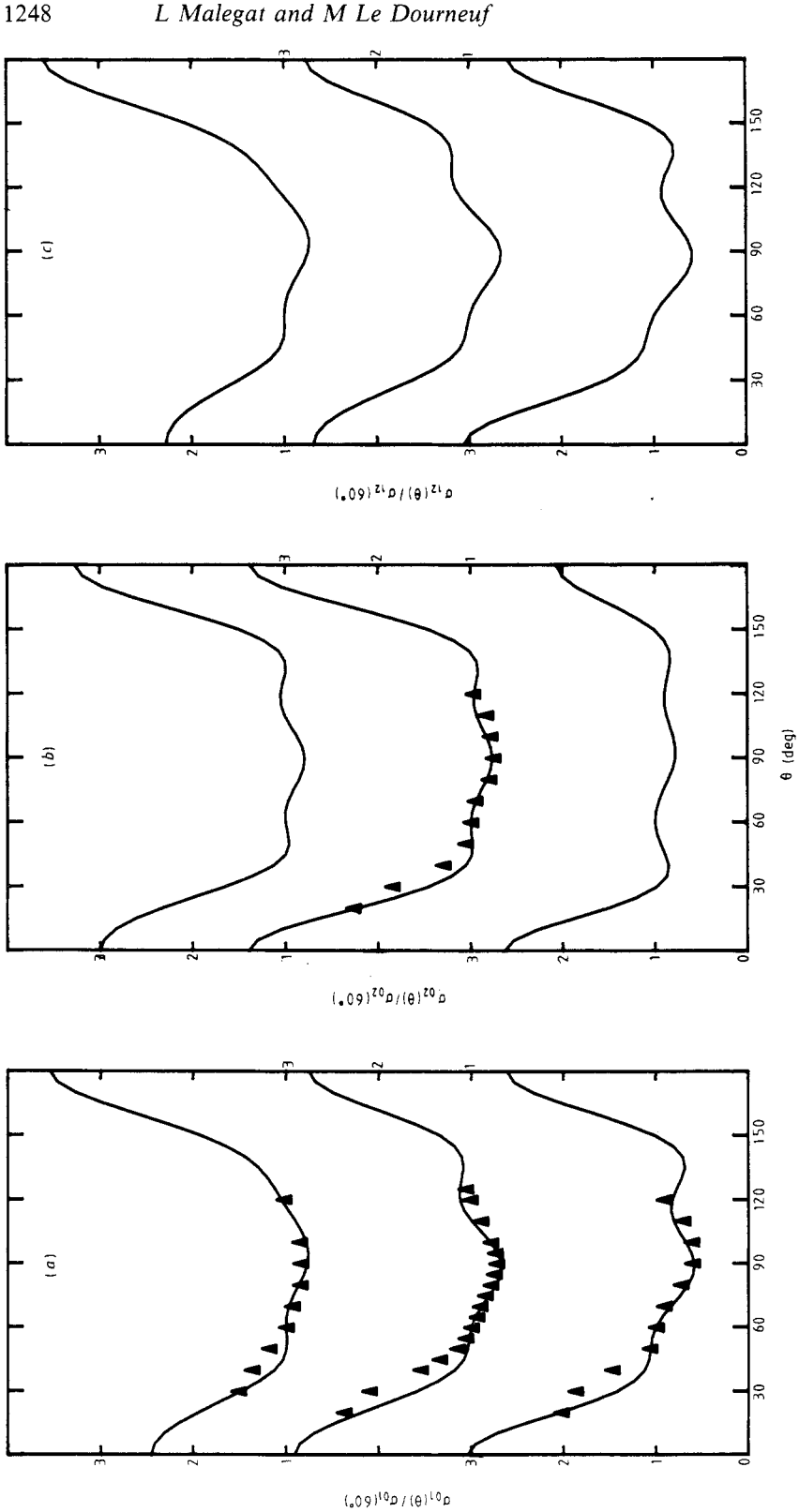

Figure 6. Differential cross sections for vibrational excitation. (*a*) $\sigma_{01}(\theta)/\sigma_{01}(60°)$ against θ in degrees for the reduced energies −1.2, 0.0, and +1.2 from lower to upper curve; (——), present work, ▲ = Tronc *et al* (1983, 1985). (*b*) Same as (*a*) but for 0→2 excitation. (*c*) Same as (*a*) but for 1→2 excitation.

Figure 6 illustrates the close agreement between our $0\rightarrow1$, $0\rightarrow2$, $1\rightarrow2$ relative vibrational DCS at three reduced energies $E_{red}=-1.2$, 0.0, +1.2 (from the lower to the upper curve), and the low-resolution measurements of Tronc *et al* (1983, 1985). The perfect symmetry of the purely resonant $0\rightarrow2$ cross section contrasts with the slight asymmetry of the $\Delta v=1$ transitions, for which we have already noticed a small non-resonant contribution in the integral cross sections (figure 3(*b*)). Moreover, their slow energy evolution is consistent with the two-wave resonant model, introduced by Chang (1977a, b), which we shall now assess in detail.

4.3. Single-parameter fitting formula for the resonant vibrational DCS

The FN elastic integrated cross sections obtained in the diabatised two-wave model differ from the exact ones by a maximal amount of the order of 0.1 a_0^2. After the R averaging, the diabatised two-channel cross section σ_{02}^{D} for the purely resonant $0\rightarrow2$ transition differs from the exact one by a maximal amount of 0.01 a_0^2, which corresponds to a relative variation of 10%. However, figure 7(*a*) shows that the corresponding DCS (dotted curve) is very close to the exact one (full curve) in the 30–140° range of experimental interest. Moreover, making the additional approximations of a constant mixing angle $\bar{\beta}=\beta(R_{eq})=(\pi/2)+(\pi/12)$ and a constant non-resonant eigenphase $\bar{\delta}=\delta(R_{eq})=\pi/2$, does not affect the diabatic result significantly.

The corresponding approximation is essentially equivalent to Chang's two-wave resonant model, which provides a single-parameter expression for the angular dependence of the resonant vibrational DCS. As a final check of this equivalence, we have calculated the DCS $\sigma_{02}^{C}(\theta)$, using Chang's equation (3) with our $\bar{\beta}$ and our $\sigma_{02}^{D}/4\pi$ as a normalisation factor (see the appendix). The unexpected disagreement between $\sigma_{02}^{D}(\theta)$ and $\sigma_{02}^{C}(\theta)$ (broken curve on figure 7(*a*)) prompted us to re-examine Chang's

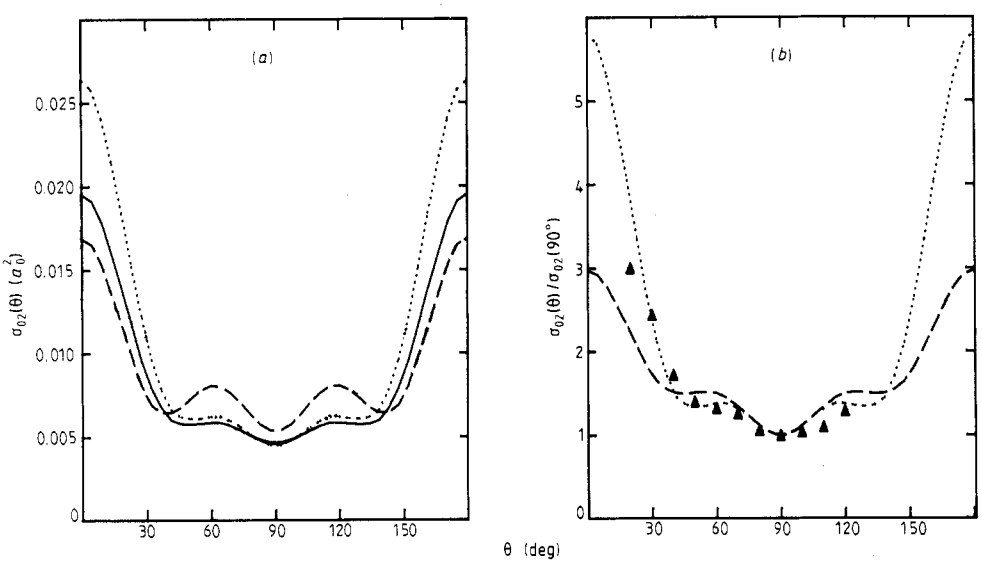

Figure 7. Adiabatic nuclei resonant two-channel scattering model. (*a*) $\sigma_{02}(\theta)$ in a_0^2 against θ in degrees at resonance; (——), present converged result; (· · · ·), present two-channel diabatised result; (- - -), Chang's (1983) equation (3), corrected for the normalisation factor. (*b*) $\sigma_{02}(\theta)/\sigma_{02}(90°)$ against θ in degrees at resonance: (· · · ·), present two-channel diabatised result; (- - -), Chang's (1983) equation (4); ▲, Tronc *et al* (1983, 1985).

calculation. Indeed, we show in the appendix that his formula omits most interference terms, owing to algebraic errors. We derive the following new expression of the vibrational excitation DCS:

$$\sigma_{v_i v_f}(\theta) = \frac{\sigma_{v_i v_f}}{4\pi}[0.150(1+\cos 2\beta)^2(1+2\cos^2\theta) + 0.178(1-\cos 2\beta)^2(1+5.68\cos^2\theta - 17.68\cos^4\theta + 14.30\cos^6\theta) + 0.133(2\sin^2 2\beta)(1-4.87\cos^2\theta + 12.50\cos^4\theta) + 0.393\sin 2\beta(1+\cos 2\beta)(1-3\cos^2\theta) + 0.083\sin 2\beta(1-\cos 2\beta)(1+12\cos^2\theta - 25\cos^4\theta)]. \quad (4)$$

Their angular variation depends on the single parameter β, the integral cross section being involved as a normalisation constant, as in Chang's original expression. The result of equation (4), using our $\bar{\beta}$ and our σ_{02}^{D} exactly reproduces the diabatised two-wave result $\sigma_{02}^{D}(\theta)$ (dotted curve on figure 7(*a*)), as it should. It yields a relative DCS (dotted curve in figure 7(*b*)) in much better agreement with Tronc's experiment (triangles) than does Chang's formula (4) (broken curve), in spite of the adjustment of β in his equation (3). In fact, this adjustment partially compensates for the lack of most interference terms, but provides a value $\beta \simeq \pi/3$ which is far from our accurate one $\bar{\beta} \simeq (\pi/2)+(\pi/12)$. Accordingly, Chang obtains a ratio of f to p amplitudes equal to 3, which is greatly underestimated compared with the present accurate value (close to 14). However, this ratio should not be given too much significance, owing to the importance of interference terms, which can be measured from the discrepancy between the dotted and broken curves on figure 7(*a*).

5. Conclusion

The present work provides extensive parameter-free results for e-N_2 scattering in the 15–35 eV range. The position and width of the fixed-nuclei $^2\Sigma_u$ electronic resonance compare well with previous results including exchange and polarisation (Dehmer *et al* 1980, Burke *et al* 1983). The fine energy mesh of our adiabatic-nuclei results points out several novel points. The integral cross sections in the various vibrational excitation channels peak at notably different energies, owing to the large width of the resonance which lets Franck-Condon factors significantly affect the shape of the resonant structures. The comparison with the total integrated cross section (Kennerly 1980) confirms that the main weakness of the present calculation, like that of previous ones, is the approximate treatment of polarisation and the neglect of electronic inelasticity. After a recalibration of the energy scale, our vibrational DCS are in excellent agreement with the relative low-resolution measurements of Tronc *et al* (1983, 1985), confirming the attribution of the vibrational excitation enhancement to a σ_u f-dominated shape resonance.

Then, the detailed analysis of our results points out the very weak coupling of two diabatised eigenphases, corresponding to a weak and practically constant mixing of p,f waves: a resonant f-dominated eigenphase and a non-resonant, p-dominated eigenphase. We thus confirm the validity of Chang's (1983) simplifying assumptions for the $N_2^-(^2\Sigma_u)$ resonance, but point out algebraic errors in his final formulae for vibrational excitation DCS in homonuclear species. We give new expressions (A4 and A5), which could be used safely by experimentalists to analyse their angular distributions: they depend only on the mixing angle β, the integral cross section acting as a normalisation factor.

Further work should therefore mainly aim at eliminating the few eV overestimation of all the resonant peak positions, by investigating omitted or incompletely included effects in the order of expected decreasing importance.

The most drastic approximation of all the available calculations is the omission of electronic excitation, although the $^2\Sigma_u$ resonance is observed much above the N_2 ionisation threshold (15.5 eV). Since it corresponds to the temporary capture of the incident electron in the σ_u valence orbital, the coupling to all the valence states of N_2 might lower its position by a few eV. Note, however, that the balance of correlation in N_2 and N_2^- would then require the inclusion of the corresponding valence-type excitations in the representation of the target states, similarly to what has been done for atoms (Le Dourneuf *et al* 1977).

Most of the dynamic polarisation should be included in such a calculation, but it may be difficult to perform with the present codes. Therefore, it remains useful to investigate further the static+exchange+polarisation approximation. The agreement between the energy shifts induced by polarisation in the present work and in that of BNS should be taken with caution. On one hand, BNS have not explicitly checked the convergence of their L^2 expansion, and perhaps not included the long range r^{-4} tail of the polarisation potential. On the other hand, the parameter-free polarisation potential we use has never been compared with more accurate approaches. However, the comparison of a similar potential with an *ab initio* (better than adiabatic dipole) polarisation potential has been performed for e-H_2 (Morrison and Saha 1986), pointing out significant variations in the magnitude of vibrational cross sections.

Target correlation effects should play a minor role, most likely shifting the resonance energy in the wrong direction. Two simple FN calculations (Rumble *et al* 1984, Weatherford *et al* 1987) support this conjecture. However, they do not ensure the balance of correlation between the N and $N+1$ electron systems, which leads to abnormally large upward shifts of their $N_2^-(^2\Pi_g)$ resonance. Therefore, a consistent inclusion of valence-type excitations in the representation of N_2 and N_2^- states cannot be performed at the static-exchange level, but should include valence-type electronic excitations.

Consequently, the elimination of the present 2-4 eV overestimation of the resonant peak positions raises two fundamental problems: the consistent description of correlation in N- and $(N+1)$-electron systems involving a partially occupied open shell, and the accurate treatment of the intermediate energy scattering. The solution of these problems should progress in parallel to similar investigations on simpler atomic systems.

Acknowledgments

We gratefully acknowledge Dr Vo Ky Lan, who stimulated the early stage of this work and provided us with his fixed-nuclei electron-molecule scattering code. The computations have been performed on the NAS 9080 and IBM 3090 computers of the Centre InterRégional de Calcul Electronique at Orsay, France.

Appendix. Two-channel simplified expression of the vibrational excitation differential cross sections for intermediate-energy resonances in homonuclear diatomic systems

Using equations (6), (7) and (11) of Chang (1977a), which assume that molecular rotation is negligible during the collision, one obtains expressions of the differential

cross section for rovibrational excitation, which contain the same geometrical $\Theta(j_t; l_i l_i' l_f l_f'; \theta)$ and dynamical $\tau^{j_t}_{v_i l_i v_f l_f}$ factors as our expression (3) of the corresponding vibrational cross sections:

$$\sigma_{v_i j_i v_f j_f}(\theta) = \frac{\pi}{k_i^2} \sum_{\substack{\bar{j}_t \\ l_i l_i' l_f l_f'}} (j_i 0 j_t 0 | j_f 0)^2 \mathrm{i}^{l_i - l_f - l_i' + l_f'} [(2l_i+1)(2l_i'+1)]^{1/2} \times \Theta(j_t; l_i l_i' l_f l_f'; \theta) \tau^{j_t}_{v_i l_i v_f l_f} \tau^{j_t}_{v_i l_i' v_f l_f'}{}^{*}. \tag{A1}$$

The summation on $\bar{j}_t$ is restricted to values satisfying the 'parity-favoured condition' $l_i + l_f + j_t$ even, which results from the conservation of the total parity $(-1)^{l_i + j_i} = (-1)^{l_f + j_f}$ and the selection rule on rotational transitions, $j_i + j_f + j_t$ even, implied by $(j_i 0 j_t 0 | j_f 0)$. In his 1977 and 1983 papers, Chang derives explicit expressions of (A1) for resonant scattering, which involves the contribution of a single body-frame symmetry. He successively considers the low-energy homonuclear case which can be described by a single partial wave, the low-energy heteronuclear case which requires two consecutive waves l_1, l_2 and finally, in 1983, the intermediate-energy homonuclear case which requires two waves l_1, l_2 of the same parity. Since Chang deduces the expression of the two-wave homonuclear case from the two-wave heteronuclear one, we consider this case first.

The symmetry properties of the $3j$ and $6j$ coefficients, those of the reduced transition matrices and the 'parity-favoured' condition imply that the terms involved in the multiple summation of (A1) are globally invariant by simultaneous exchange of l_f with l_i and l_f' with l_i', or alternatively l_i with l_i' and l_f with l_f'. This symmetry allows us to reduce the number $2^4 = 16$ of distinct terms in the quadruple summation over the incident electron angular momenta. These terms can be grouped as follows. Four identical angular momenta appear in two of them, which are distinct. Three identical ones are present in eight others: in the heteronuclear case where l_1, l_2 have opposite parities, these terms are eliminated by the condition that $l_i + l_i'$ and $l_f + l_f'$ must have the same parity, imposed by the $3j$ coefficients occurring in the standard angular functions. Two pairs of identical momenta occur in the six remaining ones, which are reduced to three distinct ones by symmetry. Consequently, only five distinct terms remain in (A1) for heteronuclear systems at low energy.

The vibrational transition matrix $T^{\lambda}_{v_i v_f}$ is derived from the fixed-nuclei one $T^{\lambda}(R)$ using the adiabatic nuclei approximation according to (1). The two-channel $T^{\lambda}(R)$ is conveniently expressed in terms of three eigenchannel parameters, namely the resonant $\delta_r(R)$ and non-resonant $\delta_{nr}(R)$ eigenphases, and the mixing angle $\beta(R)$ which defines the two orthogonal eigenchannels by rotation of the l_1, l_2 partial waves:

$$T^{\lambda}(R) = \begin{pmatrix} \cos^2\beta(R)[\mathrm{e}^{2\mathrm{i}\delta_r(R)} - 1] + \sin^2\beta(R)[\mathrm{e}^{2\mathrm{i}\delta_{nr}(R)} - 1] & \cos\beta(R)\sin\beta(R)[\mathrm{e}^{2\mathrm{i}\delta_r(R)} - \mathrm{e}^{2\mathrm{i}\delta_{nr}(R)}] \\ \cos\beta(R)\sin\beta(R)[\mathrm{e}^{2\mathrm{i}\delta_r(R)} - \mathrm{e}^{2\mathrm{i}\delta_{nr}(R)}] & \sin^2\beta(R)[\mathrm{e}^{2\mathrm{i}\delta_r(R)} - 1] + \cos^2\beta(R)[\mathrm{e}^{2\mathrm{i}\delta_{nr}(R)} - 1] \end{pmatrix}. \tag{A2}$$

The essential approximation introduced by Chang is to neglect the R dependence of δ_{nr} and β. The vibrational T matrix is then written

$$T^{\lambda}_{v_i v_f} = \tfrac{1}{2}\tau_{v_i v_f} \begin{pmatrix} 1 + \cos 2\beta & \sin 2\beta \\ \sin 2\beta & 1 - \cos 2\beta \end{pmatrix} \tag{A3a}$$

with

$$\tau_{v_i v_f} = \int \mathrm{d}R\, \chi_{v_i}(R) \mathrm{e}^{2\mathrm{i}\delta_r(R)} \chi_{v_f}(R). \tag{A3b}$$

After some manipulations which use the symmetry properties of the $3j$ coefficients, the 'parity-favoured condition', and the opposite parities of l_1, l_2, we recover the formula (21) given by Chang (1977a), and applied by him (1977b) to the rovibrational excitation of CO.

The important point is that Chang (1983) starts from this formula (21) to study the intermediate-energy resonances in homonuclear systems, in which case the two partial waves l_1, l_2 have the same parity. In fact, the above derivation must be reconsidered from the start. In particular, the eight terms involving three equal angular momenta are now allowed: they are reduced to two distinct ones by symmetry. In addition, some sign changes in the final manipulations lead to the following replacement for his formula (21):

$$\begin{aligned}\sigma_{v_i j_i v_f j_f}(\theta) = \frac{\sigma_{v_i v_f}}{2(1+\delta_{\lambda 0})} \sum_{\text{even } j_t} (j_i 0 j_t 0 | j_f 0)^2 [&(1+\cos 2\beta)^2 (l_1 \lambda j_t 0 | l_1 \lambda)^2 \Theta(j_t; l_1 l_1 l_1 l_1; \theta) \\ &+(1-\cos 2\beta)^2 (l_2 \lambda j_t 0 | l_2 \lambda)^2 \Theta(j_t; l_2 l_2 l_2 l_2; \theta) \\ &-2 \sin^2 2\beta (l_1 \lambda j_t 0 | l_1 \lambda)(l_2 \lambda j_t 0 | l_2 \lambda) \Theta(j_t; l_1 l_1 l_2 l_2; \theta) \\ &+2 \sin^2 2\beta (l_2 \lambda j_t 0 | l_1 \lambda)^2 \Theta(j_t; l_1 l_1 l_2 l_2; \theta) \\ &-2 \sin^2 2\beta (l_1 \lambda j_t 0 | l_2 \lambda)(l_2 \lambda j_t 0 | l_1 \lambda) \Theta(j_t; l_1 l_2 l_2 l_1; \theta) \\ &-4 \sin 2\beta (1+\cos 2\beta)(l_1 \lambda j_t 0 | l_1 \lambda)(l_2 \lambda j_t 0 | l_1 \lambda) \Theta(j_t; l_1 l_1 l_1 l_2; \theta) \\ &-4 \sin 2\beta (1-\cos 2\beta)(l_2 \lambda j_t 0 | l_2 \lambda)(l_1 \lambda j_t 0 | l_2 \lambda) \Theta(j_t; l_2 l_2 l_2 l_1; \theta)]\end{aligned} \tag{A4a}$$

where $\sigma_{v_i v_f}$ is the integrated vibrational excitation cross section, related to $\tau_{v_i v_f}$ by

$$\sigma_{v_i v_f} = \frac{\pi}{k_{v_i}^2} \left(\frac{2}{1+\delta_{\lambda 0}} \right) |\tau_{v_i v_f}|^2. \tag{A4b}$$

As a result of the parity change for $l_1 + l_2$ when passing from the heteronuclear to the homonuclear case, (A4) differs from equation (21) restricted to even values of j_t in two respects.

(1) The third term has the opposite sign: this implies that its cancellation with the fifth term, reported by Chang (1977a) for the heteronuclear case, no longer occurs.

(2) Two new interference terms, corresponding to three equal angular momenta in (A1), arise.

Finally, the improper account of the parity change for $l_1 + l_2$ has led Chang to miss four of the five interference terms.

Consider now the explicit case of intermediate-energy σ_u resonances, such as the $N_2^-(^2\Sigma_u)$ case studied in the present paper. After averaging over the rotation, which eliminates the Clebsh-Gordan coefficient containing the rotational dependence, and introducing the explicit angular factors for the p,f partial waves, the vibrational excitation cross sections read

$$\begin{aligned}\sigma_{v_i v_f}(\theta) = \frac{\sigma_{v_i v_f}}{4\pi} [&0.150(1+\cos 2\beta)^2 (1+2\cos^2\theta) \\ &+0.178(1-\cos 2\beta)^2 (1+5.68\cos^2\theta - 17.68\cos^4\theta + 14.30\cos^6\theta) \\ &+0.133(2\sin^2 2\beta)(1-4.87\cos^2\theta + 12.50\cos^4\theta) \\ &+0.393 \sin 2\beta (1+\cos 2\beta)(1-3\cos^2\theta) \\ &+0.083 \sin 2\beta (1-\cos 2\beta)(1+12\cos^2\theta - 25\cos^4\theta)].\end{aligned} \tag{A5}$$

Equation (A5) differs from equation (3) of Chang (1983) in two important respects.

(1) The interference term in $\sin^2 2\beta$ consists of three components, the first and the third of which cancelled wrongly in the work of Chang.

(2) The last two interference terms are missing from the start in Chang's calculation. Two minor points can also be pointed out.

(*a*) The $1/4\pi$ normalisation factor is omitted by Chang who alternatively uses the true integrated $\sigma_{v_i v_f}$ cross section or introduces an average angular cross section $\bar{\sigma}_{v_i v_f} = \sigma_{v_i v_f}/4\pi$. This is not of much consequence, since Chang'e expressions are currently used within a normalisation factor.

(*b*) The determination of β. In (A2), Chang assumes that the resonant eigenphase is l_1. Therefore, for high-l intermediate-energy resonances, a mixing angle of $\pi/2$ corresponds to a pure l_2 resonance, and a small departure from this value to a small constant admixture of l_1 in the resonant eigenphase.

References

Burke P G 1987 Private communication
Burke P G, Cooper J and Ormonde S 1969 *Phys. Rev.* **183** 245
Burke P G, Noble C J and Salvini S 1983 *J. Phys. B: At. Mol. Phys.* **16** L113
Chang E S 1977a *Phys. Rev.* A **16** 1841
—— 1977b *Phys. Rev.* A **16** 1850
—— 1983 *Phys. Rev.* A **27** 709
Chase D M 1956 *Phys. Rev.* **104** 838
Dehmer J L, Siegel J, Welch J and Dill D 1980 *Phys. Rev.* A **21** 101
Dill D and Dehmer J L 1977 *Phys. Rev.* A **16** 1423
Fano U and Dill D 1972 *Phys. Rev.* A **6** 185
Kennerly R E 1980 *Phys. Rev.* A **21** 1876
Launay J M 1987 Private communication
Le Dourneuf M and Vo Ky Lan 1977 *J. Phys. B: At. Mol. Phys.* **10** L35
Le Dourneuf M, Vo Ky Lan and Burke P G 1977 *Comment. At. Mol. Phys.* **7** 1
Lofthus A 1960 *Spectroscopic Report No* 2 University of Oslo
Malegat L, Le Dourneuf M and Vo Ky Lan 1987 *J. Phys. B: At. Mol. Phys.* **20** 4143
Morrison M A and Collins L A 1978 *Phys. Rev.* A **17** 918
Morrison M A and Hay P J 1979 *J. Chem. Phys.* **70** 4034
Morrison M A and Saha B C 1986 *Phys. Rev.* A **34** 2786
Nesbet R K 1964 *J. Chem. Phys.* **40** 3619
—— 1979 *Phys. Rev.* A **19** 551
O'Connell J K and Lane N F 1983 *Phys. Rev.* A **27** 1893
Padial N T and Norcross D W 1984 *Phys. Rev.* A **29** 1742
Pavlovic Z, Boness M J W, Herzenberg A and Schulz G J 1972 *Phys. Rev.* A **6** 676
Rumble J R, Stevens W J and Truhlar D G 1984 *J. Phys. B: At. Mol. Phys.* **17** 3151
Rumble J R, Truhlar D G and Morrison M A 1981 *J. Phys. B: At. Mol. Phys.* **14** L301
Tanaka H, Yamamoto T and Okada T 1981 *J. Phys. B: At. Mol. Phys.* **14** 2081
Tronc M 1983 Private communication
Tronc M, Azria R and Le Coat Y 1980 *J. Phys. B: At. Mol. Phys.* **13** 2327
Tronc M and Malegat L 1985 *Proc. 38th Int. Mtg on Photophysics and Photochemistry above 6 eV* ed F Lahmani (Amsterdam: Elsevier) p 203
Vo Ky Lan 1984 Private communication
Vosko S H, Wilk L and Nusair M 1980 *Can. J. Phys.* **58** 1200
Weatherford C A, Brown F B and Temkin A 1987 *Phys. Rev.* A **35** 4561
Wigner E P 1955 *Phys. Rev.* **98** 145